Society of Medical Education & Research

2021, Volume 1, Page No: 177-188
ISSN: 3108-4826

Journal of Medical Sciences and Interdisciplinary Research

Quantitative T1 Mapping Reveals Alterations in Cortical Microstructure Across Schizophrenia Spectrum Disorders

Maria Alessandra Ricci[1]*, Francesca Paola Greco[1]

[1]Department of Management, LUISS Guido Carli University, Rome, Italy.

***E-mail** ✉ m.ricci.luiss@gmail.com

Abstract

Alterations of the cerebral cortex are a well-documented feature of schizophrenia spectrum disorders (SSD), with frontal and temporal regions being particularly affected. Despite this, the majority of prior neuroimaging research has emphasized macrostructural characteristics—such as cortical thickness, volume, and surface area—rather than properties at the tissue microstructural level. Quantitative T1 (qT1) imaging enables in vivo assessment of cortical microstructure and is thought to predominantly reflect variations in myelin content.

The study included fourteen individuals diagnosed with SSD and seven demographically comparable healthy controls. All participants underwent qT1 imaging using two acquisition approaches: a single-echo protocol and a multi-echo protocol.

After adjusting for age and sex, individuals with SSD exhibited significantly higher qT1 values in frontal and temporal cortices relative to controls. This effect was observed exclusively with the single-echo qT1 acquisition. Furthermore, within the SSD group, sex exerted a modulatory effect on qT1 measures, such that female patients showed lower qT1 values than male patients when assessed with the single-echo protocol.

The findings are consistent with disrupted cortical myelination in frontal and temporal regions in SSD. In addition, the results underscore the critical role of acquisition protocol choice, as discrepancies between qT1 methods remain evident despite advances aimed at improving the quantitative robustness of these techniques.

●Extensive cortical abnormalities are evident in schizophrenia spectrum disorders, particularly within frontotemporal regions.

●Increased qT1 values indicate reduced cortical myelination in individuals with SSD.

●Methodological choices in qT1 acquisition substantially influence observed outcomes, emphasizing the need for careful protocol selection.

Keywords: Schizophrenia, Neuropsychiatry, Neuroimaging, Multimodal imaging, MRI, Quantitative T1 mapping

Introduction

Since the earliest applications of neuroimaging in psychiatry, abnormalities of the cerebral cortex have been recognized as a core feature of schizophrenia spectrum disorders (SSD). Magnetic resonance imaging (MRI) studies, in particular, have consistently identified cortical alterations as a defining aspect of the disorder [1]. Among the most robust findings are reductions in cortical thickness affecting frontal and temporal regions when SSD patients are compared with healthy individuals [2, 3]. Additional investigations have reported atypical cortical folding patterns, although results regarding the direction and extent of these changes remain inconsistent [4–6]. While these

Access this article online https://smerpub.com/

Received: 05 August 2021; **Accepted:** 25 November 2021

How to cite this article: Ricci MA, Greco FP. Quantitative T1 Mapping Reveals Alterations in Cortical Microstructure Across Schizophrenia Spectrum Disorders. J Med Sci Interdiscip Res. 2021;1:177-88. https://doi.org/10.51847/3ntaK3QPyE

macrostructural observations have greatly advanced understanding of SSD-related brain alterations, they largely reflect gross anatomical differences and have limited translational relevance.

At the microstructural level, evidence has traditionally been derived from post-mortem investigations. These studies have repeatedly demonstrated decreases in neuronal size and alterations in the density of inhibitory interneurons within the cortex of individuals with SSD [7]. Moreover, immunohistochemical analyses have revealed reductions in both the number and density of oligodendrocytes in frontal and parietal cortical regions, particularly Brodmann areas 10 and 39 [8–10]. Complementary molecular findings indicate diminished expression of myelin-associated genes in the anterior cingulate cortex [11]. Although demyelination has classically been associated with white matter pathology, such observations suggest that cortical myelin is also compromised in SSD. Nonetheless, post-mortem approaches are constrained by limited sample sizes and an inability to adequately control for clinical and demographic confounders. In vivo characterization of cortical myelin has been relatively limited, largely because quantitative, non-invasive myelin-sensitive imaging techniques have only recently become widely available.

Early in vivo efforts include the use of transverse relaxation time (T2) mapping as an indirect marker of myelin content in schizophrenia [12]. More recently, whole-cortex myelin mapping using T1-weighted/T2-weighted (T1w/T2w) ratios has been applied in first-episode psychosis cohorts [13, 14]. However, investigations focusing on cortical microstructure beyond white matter, particularly in chronic SSD populations, remain sparse. Among available quantitative approaches, longitudinal relaxation time mapping—commonly referred to as quantitative T1 (qT1)—has demonstrated advantages over alternative techniques, including reduced inter- and intra-subject variability and improved contrast-to-noise characteristics [15]. Although qT1 values are influenced by multiple biological factors, such as cellular density, iron content, and water composition [16], converging evidence suggests that myelin content is the dominant determinant [17–19].

In earlier work, we reported elevated qT1 values in subcortical structures of individuals with SSD [20]. That study also examined the sensitivity and reliability of different qT1 acquisition strategies, specifically comparing single-echo and multi-echo fast spoiled gradient echo (fSPGR) sequences. The multi-echo approach is particularly appealing because it allows simultaneous generation of several imaging contrasts, including qT1, T1-weighted, T2*, quantitative susceptibility mapping (QSM), and susceptibility-weighted imaging (SWI) [4, 21–23]. Such multimodal acquisitions are especially advantageous in psychiatric research, where longer scanning protocols may be poorly tolerated due to symptom severity or agitation. By reducing total scan time and minimizing the need for multiple acquisitions and subsequent image co-registration, multimodal imaging may also help address longstanding reproducibility challenges in neuroimaging research [24, 25]. Nevertheless, different acquisition protocols may vary in their sensitivity to microstructural alterations and in their susceptibility to influences such as age, sex, or antipsychotic treatment. Accordingly, the present study aimed to characterize cortical qT1 alterations in SSD relative to healthy controls and to evaluate the extent of inter-protocol variability between single-echo and multi-echo qT1 acquisitions.

Materials and Methods

Participants and recruitment

Fourteen individuals meeting diagnostic criteria for schizophrenia spectrum disorders and seven healthy control participants were enrolled through the Centre for Addiction & Mental Health (CAMH) in Toronto. Diagnoses in the SSD group were established using the Mini-International Neuropsychiatric Interview (MINI) based on DSM-5 criteria [26]. Healthy controls had no history of psychotic disorders, while all SSD participants were receiving antipsychotic medication at the time of the study. Exclusion criteria for both groups included traumatic brain injury, substance-induced psychosis, intellectual disability, and major neurological conditions. Within the SSD cohort, two participants were diagnosed with schizoaffective disorder, and the remainder with schizophrenia. Although the SSD group was older on average, the groups were comparable with respect to sex distribution and ethnicity. Detailed demographic characteristics are provided in **Table 1.**

Table 1. Demographic breakdown of study participants.

Demographic Variable	P-value	HC (n=7)	SD (n=14)

Age (years)	0.0009	28 ± 9.30	47 ± 14
% Male	0.875	57	57
% Caucasian	0.117	14.29	46.67
Chlorpromazine equivalents (CPZe)	–	–	548 ± 320

MRI acquisition parameters

Imaging data were collected on a 3 Tesla GE MRI system equipped with a built-in RF body transmitter and an 8-channel phased-array head coil (GE Healthcare, Waukesha, WI). Quantitative T1 (qT1) measurements were obtained using two distinct acquisition strategies. The first consisted of a sagittal single spoiled gradient echo sequence acquired at two flip angles (3° and 14°), with an echo time of 4.948 ms and isotropic spatial resolution of 1 mm^3; this approach is referred to as the single-echo qT1 (SE-qT1). The second approach employed an axial fast spoiled gradient echo sequence with 2 flip angles (3° and 24°), five echoes (initial TE = 3.36 ms, echo spacing = 4.42 ms, repetition time = 28.5 ms), and a voxel size of 0.5 × 0.5 × 2 mm^3, and is termed the multi-echo qT1 (ME-qT1).

To compensate for transmit field (B1) non-uniformities, a fast spin echo double-angle method (FSE-DAM) was implemented following the procedure described by Samson *et al*. [27]. This involved acquiring two multi-slice sagittal FSE datasets (TR = 15 s, effective TE = 14 ms, echo train length = 8) using excitation angles of 60° and 120°. In addition, high-resolution anatomical images were acquired to support cortical surface reconstruction using a standard sagittal T1-weighted BRAVO sequence (flip angle = 8°, TR = 6.868 ms, TE = 3.016 ms, inversion time = 650 ms), with a voxel resolution of 0.9 mm^3.

T1 map generation and processing

Quantitative T1 maps were computed in line with the methodology outlined by Nader *et al*. [20]. For the ME-qT1 protocol, signal intensities from the five echoes were first averaged separately for each flip angle. All qT1 datasets were registered to a halfway space, after which B1 correction factors were derived and scaled using a scanner-specific constant to generate B1 maps [28]. These maps were applied to correct voxel-wise flip angle deviations, and T1 relaxation times were subsequently estimated by fitting the spoiled gradient echo signal model.

Cortical surface reconstruction and segmentation were performed on the T1-weighted anatomical images using FreeSurfer version 7.1.1 via the automated recon-all pipeline [29]. Cortical regions were defined according to the Desikan–Killiany atlas [30]. Visual inspection confirmed satisfactory surface reconstruction, requiring only minor manual adjustments related to intensity normalization and correction of pial surface inaccuracies. Individual qT1 volumes were then sampled onto the cortical mid-surface using FreeSurfer's mri_vol2surf utility with a projection fraction of 0.5.

Statistical analysis

Initial analyses examined the correspondence between SE-qT1 and ME-qT1 values within each region of interest (ROI) using correlation testing. All subsequent analyses were conducted independently for each acquisition protocol. For visualization of group differences, vertex-wise qT1 data were normalized to FreeSurfer's fsaverage template using mris_preproc and displayed as surface maps. ROI-level group comparisons were performed by extracting mean qT1 values per region and assessing differences between SSD and control groups using general linear models implemented with the lm function in R, controlling for age and sex [31]. Within the SSD cohort, additional covariate analyses evaluated the sensitivity of each protocol to age, sex, and chlorpromazine equivalent dose (CPZe), while adjusting for the remaining covariates. Correction for multiple testing was applied using the Benjamini–Hochberg false discovery rate (FDR) procedure, and all statistical tests were conducted separately for the left and right hemispheres.

Results and Discussion

Inter-protocol qT1 correlation

The relationship between SE-qT1 and ME-qT1 measurements was first assessed across cortical ROIs. After controlling for multiple comparisons, significant associations in the left hemisphere were limited to six regions: the isthmus of the cingulate gyrus, fusiform gyrus, middle temporal cortex, cuneus, lateral occipital cortex, and pericalcarine area **(Figure 1a).** In contrast, no cortical regions in the right hemisphere demonstrated significant correlations between the two qT1 protocols following correction for multiple comparisons **(Figure 1b).**

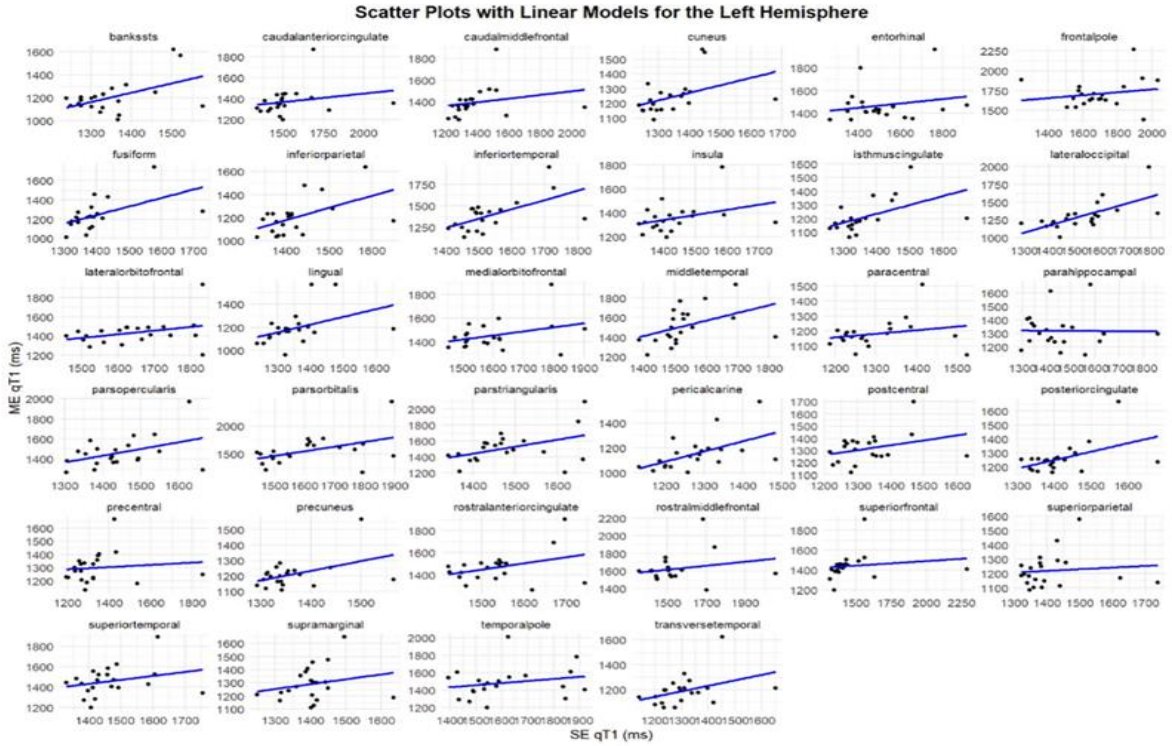

a)

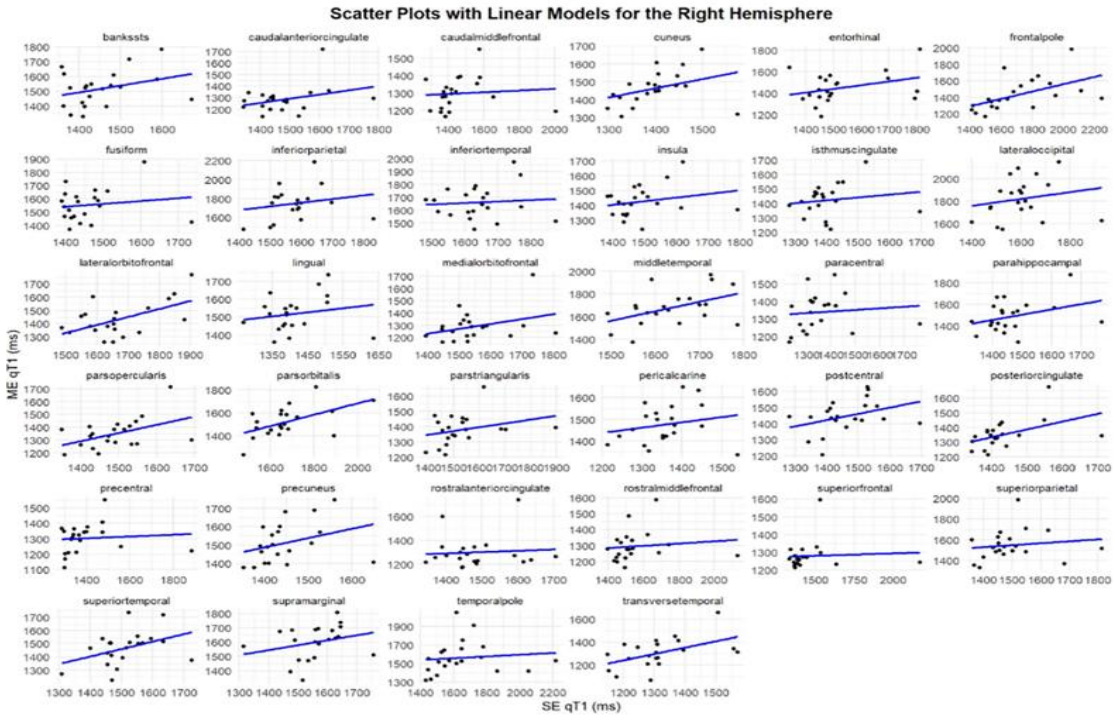

b)

Figure 1. Heterogeneous correlations between SE-qT1 and ME-qT1 across cortical regions of interest. Each point corresponds to an individual participant, and the fitted line represents the linear regression across all subjects (n = 21). SE-qT1 denotes single-echo quantitative T1, while ME-qT1 denotes multi-echo quantitative T1.

Cortical microstructural alterations in SSD

Group-related differences in cortical qT1 were examined by projecting individual maps onto a shared surface template and computing vertex-wise contrasts between schizophrenia spectrum disorder (SSD) participants and healthy controls (HC) **(Figure 2)**. In general, both qT1 acquisition strategies revealed elevated qT1 values in the SSD group relative to controls, with the most prominent increases observed in the left frontal and temporal cortices and extending into right-sided temporoparietal regions **(Figure 2).** In contrast, reductions in qT1 among SSD patients were limited to a small number of parietal and occipital areas and appeared spatially restricted **(Figure 2).** Notably, the ME-qT1 protocol yielded changes that were broader in extent and less spatially focal than those detected with SE-qT1, most clearly illustrated by the widespread alterations observed in the right temporoparietal cortex **(Figure 2).**

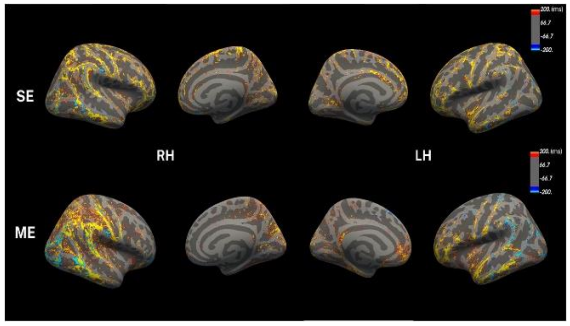

Figure 2. Cortical qT1 contrasts between individuals with schizophrenia spectrum disorders (SSD) and healthy controls (HC). Vertex-wise maps represent SSD–HC differences and are presented for descriptive purposes only; the color scale indicates qT1 values in milliseconds (ms). Identical visualization procedures were applied to both acquisition protocols (SSD: n = 14; HC: n = 7).

To characterize region-specific effects, mean qT1 values were extracted for each cortical parcel and compared between groups. When raw group comparisons were performed without covariate adjustment, no regional differences survived correction for multiple testing. In contrast, models that accounted for age and sex revealed a distinct pattern limited to the single-echo qT1 (SE-qT1) protocol, which demonstrated significantly higher qT1 values in the SSD group relative to controls **(Figure 3).** These alterations were distributed across frontal, temporal, parietal, and occipital cortices, with effect sizes varying from moderate in the left medial orbitofrontal region (0.59) to large in the right cuneus (1.59) **(Figure 3; Table 2)**. No statistically reliable case–control differences were identified using the multi-echo qT1 (ME-qT1) approach. Additionally, variability in qT1 measurements was notably greater for ME-qT1 than for SE-qT1, as reflected by larger standard deviations across regions **(Figure 4).**

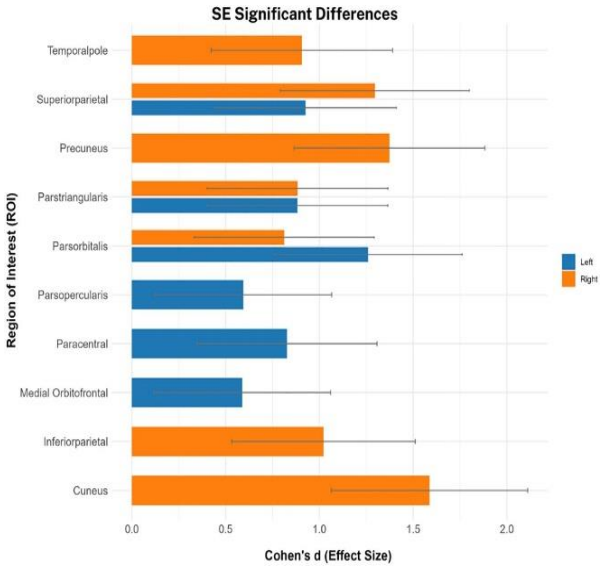

Figure 3. Region-of-interest–level qT1 differences between schizophrenia spectrum disorder (SSD) participants and healthy controls. The bar chart displays only those cortical parcels that showed statistically significant effects

using the single-echo qT1 (SE-qT1) protocol after controlling for age and sex and applying false discovery rate correction (FDR-adjusted $p < 0.05$). Error bars represent the standard error of the mean (SSD: n = 14; HC: n = 7).

Table 2. Case-control differences for SE-qT1.

Region of Interest	SSD – HC mean difference (ms) (mean ± standard error)	Effect size (Cohen's D ± standard error)	FDR-adjusted p-value
Right hemisphere			
R-temporal pole	171.05 ± 87.30	0.9 ± 0.48	0.037
R-superior parietal gyrus	120.54 ± 43.06	1.3 ± 0.50	0.021
R-inferior parietal gyrus	80.76 ± 36.58	1.02 ± 0.49	0.037
R-pars triangularis	95.31 ± 49.95	0.88 ± 0.48	0.037
R-pars orbitalis	110.8 ± 63.16	0.81 ± 0.48	0.037
R-precuneus gyrus	81.76 ± 27.55	1.37 ± 0.51	0.021
R-cuneus gyrus	85.90 ± 25.05	1.59 ± 0.52	0.021
Left hemisphere			
L-superior parietal gyrus	88.93 ± 44.45	0.93 ± 0.48	0.049
L-pars triangulairs	82.00 ± 43.03	0.88 ± 0.48	0.049
L-pars orbitalis	158.38 ± 58.21	1.26 ± 0.50	0.049
L-pars opercularis	56.23 ± 43.88	0.59 ± 0.47	0.049
L-paracentral gyrus	73.79 ± 41.29	0.83 ± 0.48	0.049
L-medial orbitofrontal gyrus	72.12 ± 56.78	0.59 ± 0.47	0.049

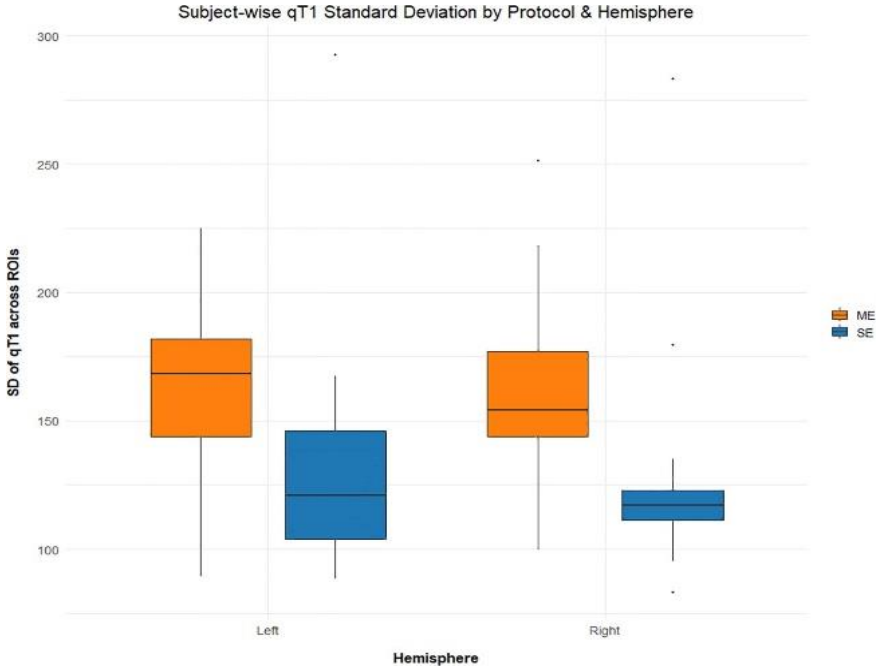

Figure 4. Hemispheric comparison of mean qT1 variability for each acquisition protocol. The boxplot illustrates the average standard deviation of qT1 values, calculated across all cortical regions of interest and pooled across participants (SSD: n = 14; HC: n = 7).

Covariate analysis of qT1 values in SSD

Finally, we assessed how each qT1 acquisition method was influenced by demographic and clinical variables within the SSD cohort, specifically age, sex, and chlorpromazine-equivalent dose (CPZe). For the single-echo qT1 (SE-qT1) protocol, sex emerged as a significant modulator, with female patients exhibiting lower qT1 values than male patients after controlling for age and CPZe. These effects were most pronounced in bilateral frontal and temporal cortices, with weaker associations extending into parietal and occipital regions **(Figure 5).** In contrast, the multi-echo qT1 (ME-qT1) protocol demonstrated a negative association with CPZe after adjustment for age and sex, confined to the right pars triangularis and lateral orbitofrontal cortex **(Figure 6).** No statistically significant covariate effects were detected in the left hemisphere using the ME-qT1 approach.

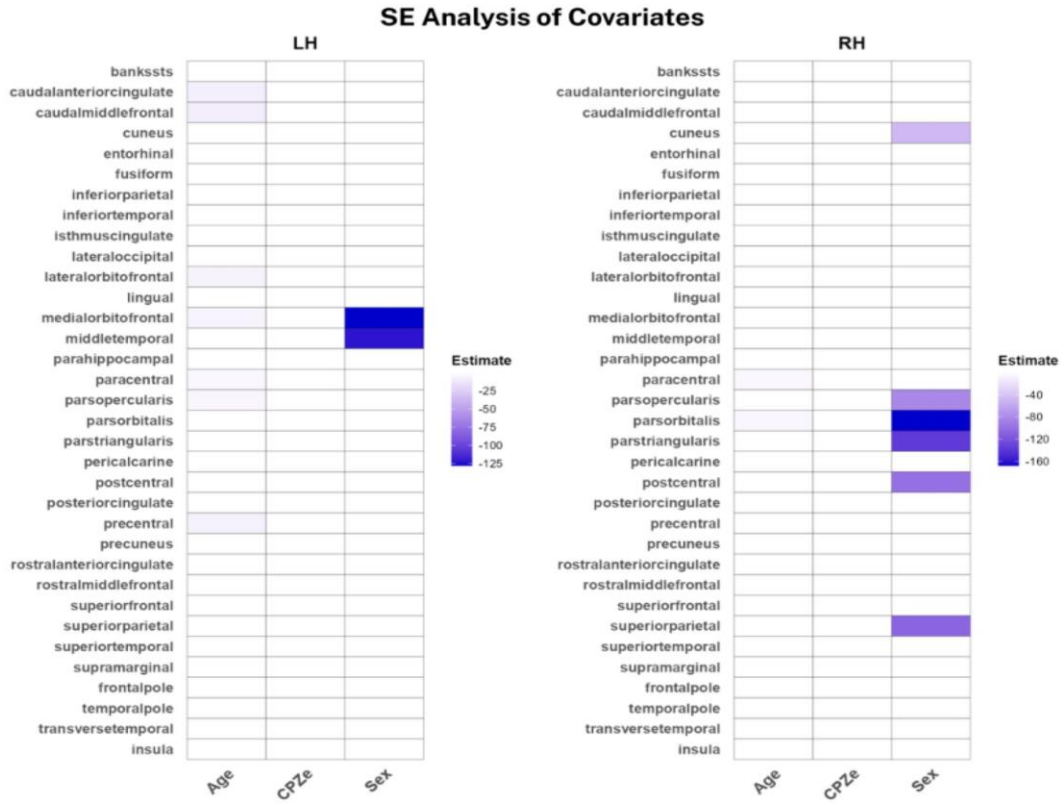

Figure 5. Heatmap representation of significant covariate effects on SE-qT1 measurements. Colored cells denote cortical regions where qT1 values showed a statistically significant association with the tested covariates, with the color scale reflecting the corresponding linear regression coefficients. For clarity, only significant effects are displayed, while non-significant associations are set to zero in the visualization (n = 14).

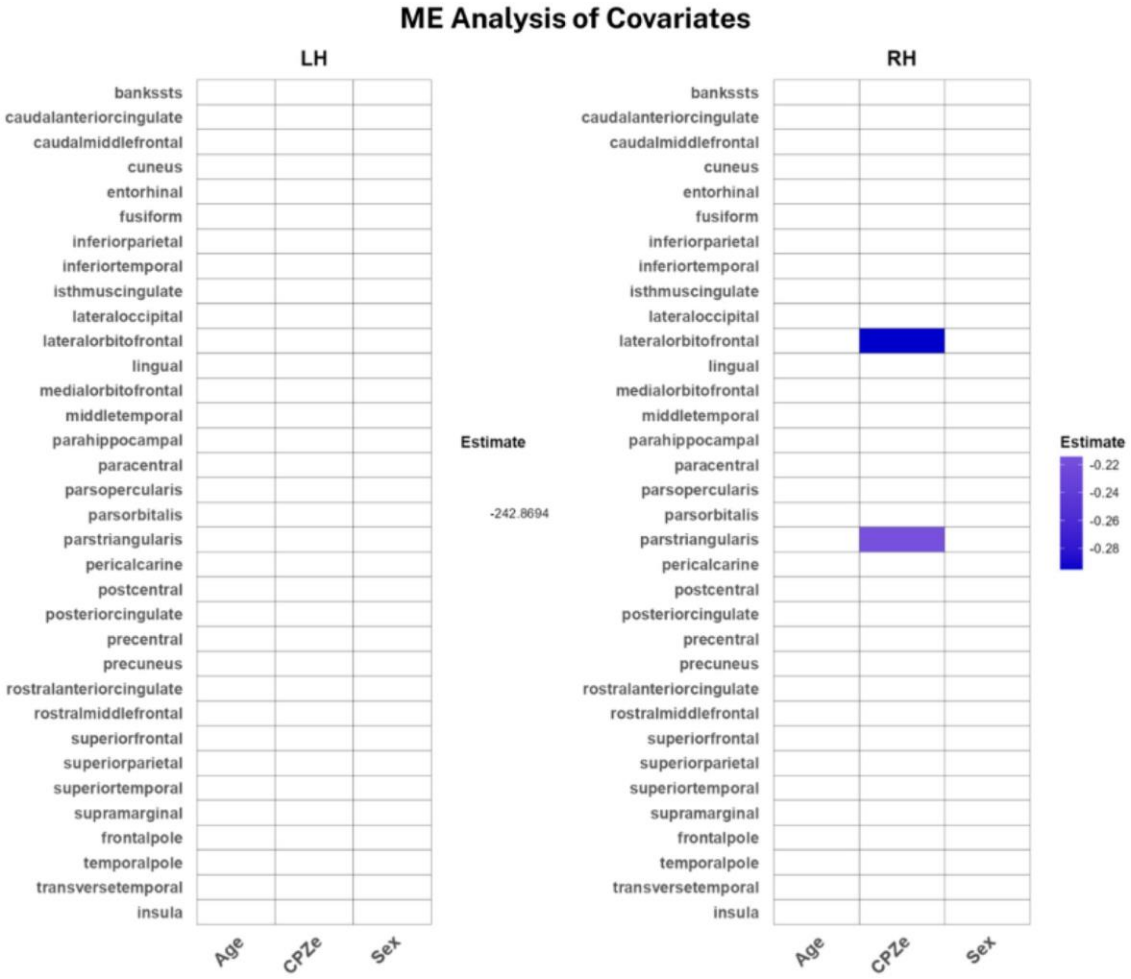

Figure 6. Heatmap depiction of significant covariate associations identified with the ME-qT1 protocol. Colored cells indicate cortical regions where qT1 values showed a statistically meaningful relationship with the examined covariates, with the color scale reflecting the corresponding regression coefficients. For clarity, only significant effects are visualized, whereas non-significant associations are set to zero (n = 14).

This study provides new in vivo evidence of cortical microstructural alterations in schizophrenia spectrum disorders (SSD) using quantitative T1 (qT1) imaging, while also directly comparing the performance and reliability of two acquisition strategies: single-echo qT1 (SE-qT1) and multi-echo fast spoiled gradient echo qT1 (ME-qT1). To our knowledge, this represents the first cortical-focused investigation to contrast these two qT1 methodologies within a medicated SSD cohort, as earlier studies primarily relied on heterogeneous imaging techniques and largely examined drug-naïve or first-episode populations.

Across cortical regions, agreement between SE-qT1 and ME-qT1 measurements was generally limited. Although weak-to-moderate correlations were observed, statistically robust associations were confined to a small subset of left-hemispheric parcels, with no regions surviving correction in the right hemisphere. Given that both qT1 maps were sampled onto an identical cortical surface, these discrepancies are most plausibly attributed to differences inherent to the T1 estimation procedures rather than surface reconstruction artifacts. In our earlier work, stronger correlations were reported when qT1 values were averaged across the entire cortex rather than examined at the parcel level [20]. The current surface-based, region-specific approach likely amplified uncertainty in smaller regions, where reduced volume

can substantially degrade measurement stability and obscure inter-protocol concordance.

At the group level, individuals with SSD demonstrated elevated qT1 values relative to healthy controls, but this effect was detectable only with the SE-qT1 protocol. Increased qT1 is generally interpreted as reflecting pathological microstructural alterations, including diminished myelin content, reduced cellular or synaptic density, neuroinflammatory processes, and iron-related changes, with myelin loss considered the dominant contributor. Notably, medium-to-large effects were concentrated in inferior frontal regions, including bilateral pars orbitalis and left pars triangularis, pars opercularis, and medial orbitofrontal cortex. These findings closely align with post-mortem observations of disrupted oligodendrocyte integrity and myelination in frontal cortices [8, 9]. They are also concordant with large-scale meta-analytic evidence reporting marked reductions in cortical thickness and gray matter volume in inferior temporal and frontal regions in SSD [32, 33]. While cortical thickness and qT1 index distinct biological properties, both measures may converge in identifying regions that are particularly vulnerable to disease-related processes, potentially linked to shared genetic influences on dendritic architecture and myelin-related pathways during neurodevelopment [34].

Evidence from first-episode psychosis studies further contextualizes these results. For example, prior work reported reduced myelination in deeper layers of the inferior frontal cortex, although effects did not reach statistical significance [13]. This discrepancy is not unexpected, as cortical abnormalities are known to intensify with illness chronicity. Supporting this notion, reductions in pars orbitalis thickness have been observed in chronic schizophrenia but not in early-stage patients [33]. Beyond frontal regions, we also identified alterations in temporal pole, superior parietal cortex, cuneus, and precuneus—areas repeatedly implicated in structural MRI studies demonstrating abnormalities in gray matter volume and surface metrics [6, 33, 35, 36].

In contrast, ME-qT1 did not reveal statistically significant case–control differences, despite effect sizes comparable to those observed with SE-qT1. The absence of significance appears to stem from greater measurement variability associated with the multi-echo approach, as reflected by larger standard deviations across hemispheres. Similar patterns were observed in our previous subcortical analyses, where SE-qT1—but not ME-qT1—detected hippocampal alterations [20]. Although multi-echo acquisitions offer the advantage of generating multiple quantitative contrasts within a single scan, this benefit may come at the expense of reduced sensitivity to subtle microstructural differences. Later echoes are increasingly influenced by T2* decay, which itself is affected by iron content, free water, and other tissue properties [37]. As a result, noise may accumulate across echoes while signal gains remain limited, diminishing the overall signal-to-noise ratio. Future studies may mitigate this limitation by selectively weighting earlier echoes or excluding later echoes from T1 estimation.

Analysis of covariates within the SSD group further highlighted protocol-dependent sensitivities. Only SE-qT1 demonstrated robust associations with sex, with female patients exhibiting lower qT1 values across multiple bilateral cortical regions after accounting for age and antipsychotic dose. This pattern mirrors our prior findings in subcortical structures and suggests sex-specific differences in cortical microstructure. Age-related effects were minimal and detectable only with SE-qT1, showing a slight decrease in qT1 values—an observation that contrasts with typical age-related trends in healthy populations. This divergence may reflect the restricted age range and modest sample size, or potentially distinct aging trajectories in SSD [38]. Interestingly, ME-qT1 values were negatively associated with chlorpromazine-equivalent dose in select right frontal regions, which may reflect medication-related influences on myelination or cellular density. Given that the majority of participants were treated with second-generation antipsychotics—agents often considered less neurotoxic than first-generation compounds—this finding is biologically plausible [3, 39].

Taken together, these results support the presence of aberrant cortical myelination in SSD and underscore the modulatory role of clinical factors such as medication exposure. Beyond enhancing pathophysiological insight, qT1 mapping may hold clinical relevance. Prior work has linked regional cortical myelination to symptom dimensions, including affective and excitatory features [13]. Considering differences in illness stage between studies, it is conceivable that qT1 alterations evolve dynamically over the course of SSD, offering potential utility as a biomarker for disease progression, treatment response, or functional outcome. Importantly, qT1 measures demonstrate strong test–retest and inter-scanner reliability, making them well suited for large-scale, multi-center investigations [40]. Integration with

machine learning and advanced analytical frameworks could further expand their diagnostic and prognostic potential.

This study has several notable strengths, including its focus on cortical-specific qT1 alterations in SSD and the direct comparison of two acquisition protocols using a shared cortical surface for projection, thereby minimizing segmentation-related confounds. However, limitations must be acknowledged. The small sample size restricts statistical power and generalizability, and partial volume effects from adjacent white matter or pial surfaces cannot be fully excluded despite quality control procedures. Additionally, imperfect age matching between groups may have influenced results. Accordingly, these findings should be regarded as preliminary, serving primarily to inform methodological optimization and guide future research.

Conclusion

In summary, our findings indicate disrupted cortical microstructure and reduced myelination in schizophrenia spectrum disorders, as reflected by elevated qT1 values relative to healthy controls. We further demonstrate that single-echo qT1 acquisition exhibits greater sensitivity to these alterations than multi-echo approaches, emphasizing the critical importance of protocol selection. Given the limited existing literature, future longitudinal and outcome-focused studies are essential to clarify how qT1-based microstructural measures relate to illness trajectory and treatment effects in schizophrenia.

Acknowledgments: None

Conflict of Interest: None

Financial Support: The author(s) declared financial support was received for this work and/or its publication. This study was funded by the AFP Innovation Fund, which was awarded to VL from the Centre for Addiction & Mental Health. GN and MD were supported by the Canadian Institute of Health Research (CIHR) Canada Graduate Scholarship.

Ethics Statement: This study involving humans was approved by the Research Ethics Board (REB) of the Centre for Addiction and Mental Health (CAMH), Toronto, Ontario, Canada (approval number 097/2016). The studies were conducted in accordance with the local legislation and institutional requirements. The participants provided their written informed consent to participate in this study.

References

1. Lawrie SM, Weinberger DR, and Johnston EC eds. *Schizophrenia: From neuroimaging to neuroscience*. United Kingdom: Oxford University Press (2004). doi: 10.1093/oso/9780198525967.001.0001
2. Rosa PGP, Zugman A, Cerqueira CT, Serpa MH, De Souza Duran FL, Zanetti MV, et al. Cortical surface abnormalities are different depending on the stage of schizophrenia: A cross-sectional vertexwise mega-analysis of thickness, area and gyrification. *Schizophr Res*. (2021) 236:104–14. doi: 10.1016/j.schres.2021.08.011
3. Van Erp TGM, Walton E, Hibar DP, Schmaal L, Jiang W, Glahn DC, et al. Cortical brain abnormalities in 4474 individuals with schizophrenia and 5098 control subjects via the enhancing neuro imaging genetics through meta analysis (ENIGMA) consortium. *Biol Psychiatry*. (2018) 84:644–54. doi: 10.1016/j.biopsych.2018.04.023
4. Gao X, Yao L, Li F, Yang C, Zhu F, Gong Q, et al. The cortical hypogyrification pattern in antipsychotic-naive first-episode schizophrenia. *Cereb Cortex*. (2023) 33:7619–26. doi: 10.1093/cercor/bhad065
5. Pham TV, Sasabayashi D, Takahashi T, Takayanagi Y, Kubota M, Furuichi A, et al. Longitudinal changes in brain gyrification in schizophrenia spectrum disorders. *Front Aging Neurosci*. (2021) 13:752575. doi: 10.3389/fnagi.2021.752575
6. Spalthoff R, Gaser C, and Nenadić I. Altered gyrification in schizophrenia and its relation to other morphometric markers. *Schizophr Res*. (2018) 202:195–202. doi: 10.1016/j.schres.2018.07.014
7. Bakhshi K and Chance SA. The neuropathology of schizophrenia: A selective review of past studies and emerging themes in brain structure and cytoarchitecture. *Neuroscience*. (2015) 303:82–102. doi: 10.1016/j.neuroscience.2015.06.028
8. Kolomeets NS and Uranova NA. Reduced number of satellite oligodendrocytes of pyramidal neurons in layer 5 of the prefrontal cortex in schizophrenia. *Eur*

Arch Psychiatry Clin Neurosci. (2022) 272:947–55. doi: 10.1007/s00406-021-01353-w

9. Uranova NA, Vostrikov VM, Orlovskaya DD, and Rachmanova VI. Oligodendroglial density in the prefrontal cortex in schizophrenia and mood disorders: A study from the Stanley Neuropathology Consortium. *Schizophr Res*. (2004) 67:269–75. doi: 10.1016/S0920-9964(03)00181-6
10. Uranova NA, Vostrikov VM, and Kolomeets NS. Oligodendrocyte abnormalities in layer 5 in the inferior parietal lobule are associated with lack of insight in schizophrenia: A postmortem morphometric study. *Eur J Psychiatry*. (2015) 29:215–22. doi: 10.4321/S0213-61632015000300006
11. Dracheva S, Davis KL, Chin B, Woo DA, Schmeidler J, and Haroutunian V. Myelin-associated mRNA and protein expression deficits in the anterior cingulate cortex and hippocampus in elderly schizophrenia patients. *Neurobiol Dis*. (2006) 21:531–40. doi: 10.1016/j.nbd.2005.08.012
12. Flynn SW, Lang DJ, Mackay AL, Goghari V, Vavasour IM, Whittall KP, et al. Abnormalities of myelination in schizophrenia detected *in vivo* with MRI, and post-mortem with analysis of oligodendrocyte proteins. *Mol Psychiatry*. (2003) 8:811–20. doi: 10.1038/sj.mp.4001337
13. Wei W, Zhang Y, Li Y, Meng Y, Li M, Wang Q, et al. Depth-dependent abnormal cortical myelination in first-episode treatment-naïve schizophrenia. *Hum Brain Mapp*. (2020) 41:2782–93. doi: 10.1002/hbm.24977
14. Wei W, Yin Y, Zhang Y, Li X, Li M, Guo W, et al. Structural covariance of depth-dependent intracortical myelination in the human brain and its application to drug-naïve schizophrenia: A T1w/T2w MRI study. *Cereb Cortex*. (2022) 32:2373–84. doi: 10.1093/cercor/bhab337
15. Haast RAM, Ivanov D, Formisano E, and Uludağ K. Reproducibility and reliability of quantitative and weighted T1 and T2∗ Mapping for myelin-based cortical parcellation at 7 tesla. *Front Neuroanat*. (2016) 10:112. doi: 10.3389/fnana.2016.00112
16. Weiskopf N, Edwards LJ, Helms G, Mohammadi S, and Kirilina E. Quantitative magnetic resonance imaging of brain anatomy and *in vivo* histology. *Nat Rev Phys*. (2021) 3. doi: 10.1038/s42254-021-00326-1
17. Desmond KL, Al-Ebraheem A, Janik R, Oakden W, Kwiecien JM, Dabrowski W, et al. Differences in iron and manganese concentration may confound the measurement of myelin from R1 and R2 relaxation rates in studies of dysmyelination. *NMR Biomed*. (2016) 29:985–98. doi: 10.1002/nbm.3549
18. Stüber C, Morawski M, Schäfer A, Labadie C, Wähnert M, Leuze C, et al. Myelin and iron concentration in the human brain: A quantitative study of MRI contrast. *NeuroImage*. (2014) 93:95–106. doi: 10.1016/j.neuroimage.2014.02.026
19. Tardif CL, Schäfer A, Waehnert M, Dinse J, Turner R, and Bazin P-L. Multi-contrast multi-scale surface registration for improved alignment of cortical areas. *NeuroImage*. (2015) 111:107–22. doi: 10.1016/j.neuroimage.2015.02.005
20. Nader G, Safara S, Desmond KL, Gerretsen P, Graff A, and De Luca V. Microstructural imaging of brain changes in schizophrenia via quantitative T1 (qT1): A preliminary comparison of two acquisition protocols. *J Neural Transm*. (2025). doi: 10.1007/s00702-025-02899-y
21. Hasegawa H, Ashikaga R, Okajima K, Wakayama T, Miyoshi M, Nishimura Y, et al. Comparison of lesion enhancement between BB Cube and 3D-SPGR images for brain tumors with 1.5-T magnetic resonance imaging. *Japanese J Radiol*. (2017) 35:463–71. doi: 10.1007/s11604-017-0654-7
22. Mazzucchi S, Del Prete E, Costagli M, Frosini D, Paoli D, Migaleddu G, et al. Morphometric imaging and quantitative susceptibility mapping as complementary tools in the diagnosis of parkinsonisms. *Eur J Neurol*. (2022) 29:2944–55. doi: 10.1111/ene.15447
23. Vishaal S, Tobias C. W, and Chavez S. *Two multi-echo SPGR acquisitions for the simultaneous generation of SWI, qT1 and other parametric maps: Preliminary data* (2021). Available online at: https://archive.ismrm.org/2021/3054.html (Accessed June 11, 2025).
24. Koçak B, Yüzkan S, Mutlu S, Karagülle M, Kala A, Kadıoğlu M, et al. Influence of image preprocessing on the segmentation-based reproducibility of radiomic features: *In vivo* experiments on discretization and resampling parameters. *Diagn Interventional Radiol*. (2024) 30:152–62. doi: 10.4274/dir.2023.232543
25. Moradmand H, Aghamiri SMR, and Ghaderi R. Impact of image preprocessing methods on

reproducibility of radiomic features in multimodal magnetic resonance imaging in glioblastoma. *J Appl Clin Med Phys*. (2019) 21:179–90. doi: 10.1002/acm2.12795

26. Sheehan DV, Lecrubier Y, Sheehan KH, Amorim P, Janavs J, Weiller E, et al. The Mini-International Neuropsychiatric Interview (M.I.N.I.): The development and validation of a structured diagnostic psychiatric interview for DSM-IV and ICD-10. *J Clin Psychiatry*. (1998) 59:22–33;quiz 34-57.
27. Samson RS, Wheeler-Kingshott CAM, Symms MR, Tozer DJ, and Tofts PS. A simple correction for B1 field errors in magnetization transfer ratio measurements. *Magnetic Resonance Imaging*. (2006) 24:255–63. doi: 10.1016/j.mri.2005.10.025
28. Desmond KL, Xu R, Sun Y, and Chavez S. A practical method for post-acquisition reduction of bias in fast, whole-brain B1-maps. *Magnetic Resonance Imaging*. (2021) 77:88–98. doi: 10.1016/j.mri.2020.12.009
29. Fischl B. FreeSurfer. *NeuroImage*. (2012) 62:774–81. doi: 10.1016/j.neuroimage.2012.01.021
30. Desikan RS, Ségonne F, Fischl B, Quinn BT, Dickerson BC, Blacker D, et al. An automated labeling system for subdividing the human cerebral cortex on MRI scans into gyral based regions of interest. *NeuroImage*. (2006) 31:968–80. doi: 10.1016/j.neuroimage.2006.01.021
31. R Foundation for Statistical Computing. *R: A Language and Environment for Statistical Computing (Version 4.4.1)* (2024). R Core Team. Available online at: https://www.R-project.org/ (Accessed June 11, 2025).
32. Suzuki M, Zhou S-Y, Takahashi T, Hagino H, Kawasaki Y, Niu L, et al. Differential contributions of prefrontal and temporolimbic pathology to mechanisms of psychosis. *Brain*. (2005) 128:2109–22. doi: 10.1093/brain/awh554
33. Zhao Y, Zhang Q, Shah C, Li Q, Sweeney JA, Li F, et al. Cortical thickness abnormalities at different stages of the illness course in schizophrenia: A systematic review and meta-analysis. *JAMA Psychiatry*. (2022) 79:560–70. doi: 10.1001/jamapsychiatry.2022.0799
34. Parker N, Patel Y, Jackowski AP, Pan PM, Salum GA, Pausova Z, et al. Assessment of neurobiological mechanisms of cortical thinning during childhood and adolescence and their implications for psychiatric disorders. *JAMA Psychiatry*. (2020) 77:1127–36. doi: 10.1001/jamapsychiatry.2020.1495
35. Banaj N, Vecchio D, Piras F, De Rossi P, Bustillo J, Ciufolini S, et al. Cortical morphology in patients with the deficit and non-deficit syndrome of schizophrenia: A worldwide meta- and mega-analyses. *Mol Psychiatry*. (2023) 28:4363–73. doi: 10.1038/s41380-023-02221-w
36. Zhao C, Zhu J, Liu X, Pu C, Lai Y, Chen L, et al. Structural and functional brain abnormalities in schizophrenia: A cross-sectional study at different stages of the disease. *Prog Neuropsychopharmacol Biol Psychiatry*. (2018) 83:27–32. doi: 10.1016/j.pnpbp.2017.12.017
37. Sun H, Cleary JO, Glarin R, Kolbe SC, Ordidge RJ, Moffat BA, et al. Extracting more for less: Multi-echo MP2RAGE for simultaneous T1-weighted imaging, T1 mapping, mapping, SWI, and QSM from a single acquisition. *Magnetic Resonance Med*. (2020) 83:1178–91. doi: 10.1002/mrm.27975
38. Gräfe D, Frahm J, Merkenschlager A, Voit D, and Hirsch FW. Quantitative T1 mapping of the normal brain from early infancy to adulthood. *Pediatr Radiol*. (2021) 51:450–6. doi: 10.1007/s00247-020-04842-7
39. Thompson PM, Bartzokis G, Hayashi KM, Klunder AD, Lu PH, Edwards N, et al. Time-lapse mapping of cortical changes in schizophrenia with different treatments. *Cereb Cortex (New York NY)*. (2009) 19:1107–23. doi: 10.1093/cercor/bhn152
40. Gracien R-M, Maiworm M, Brüche N, Shrestha M, Nöth U, Hattingen E, et al. How stable is quantitative MRI? – Assessment of intra- and inter-scanner-model reproducibility using identical acquisition sequences and data analysis programs. *NeuroImage*. (2020) 207:116364. doi: 10.1016/j.neuroimage.2019.116364